Surface electronic structure of a step-well-basis superlattice

R. Kucharczyk*r and M. Stęślicka
Institute of Experimental Physics, University of Wrocław, plac Maksa Borna 9, 50-204 Wrocław, Poland

A. Akjouj, B. Djafari-Rouhani, and L. Dobrzynski
Laboratoire de Dynamique et Structure des Matériaux Moléculaires, URA CNRS No. 801, UFR de Physique, Université de Lille I, 59655 Villeneuve d'Ascq Cedex, France

E. H. El Boudouti
Département de Physique, Faculté des Sciences, Université de Oujda, Oujda, Morocco
(Received 24 March 1998)

Surface electronic structure of a semi-infinite *polytype* superlattice (SL) with period consisting of three different layers (the so-called *step-well basis*) is investigated using a transfer-matrix approach within an effective-mass approximation. Explicit analytical formulas for the bulk dispersion relation as well as the energy expression and existence condition for surface states are given for arbitrary terminating medium and their simplification for particular SL terminations by a substrate identical to one of the SL constituents is discussed. Dependence of surface-state properties (i.e., its energy position and the degree of localization) on SL parameters (i.e., layer thicknesses and potential barrier heights) and different surface configurations (depending on a sequence of SL layers approaching the surface as well as on the choice of substrate) is studied for a triple-constituent $Al_xGa_{1-x}As$-based SL. Additionally, surface-state wave functions are plotted in order to examine the associated space-charge distributions. [S0163-1829(98)04132-0]

I. INTRODUCTION

With recent advances in epitaxial growth techniques, it has become possible to grow—with sufficiently high precision—semiconductor superlattices (SL's) composed of alternating layers of more than two different materials. These so-called *polytype* or *complex-basis* SL's, initially proposed in Ref. 1, have proved to be useful for specific device purposes, as they exhibit some superior electronic, optical, and transport characteristics as compared to typical *binary* (two-layer basis) SL's. To be more specific, coupled-well and step-well bases have been proposed to improve performance of multi-quantum-well lasers, electro-optic switches, modulators, and infrared photodetectors.[2–8] A possibility of controlling the miniband and minigap widths independently in complex-basis SL's has also found application in band-aligned structures and effective-mass filters as well as in tuning of the tunneling current.[3,9–12]

Numerous bulk electronic structure calculations reported for polytype SL's (Refs. 9 and 11–17) indicate that their desired properties can be engineered owing to additional degrees of freedom that are available in a multilayer basis with respect to a two-layer basis. In reality, however, SL's consist of a finite number of periods and form interfaces with a substrate and/or a cladding layer (the so-called *internal surfaces*[18]), which give rise to Tamm-like states[19,20] confined to the SL end and located within energy minigaps. The density-of-states analysis performed for a terminated SL indicated that the occurrence of such surface states could—under certain conditions—result in a virtual nonexistence of the forbidden energy gap over a few outermost SL periods.[21,22] Thus, it is important to take into account surface effects when determining the electronic characteristics of SL's.

The existence and properties of electronic surface states in binary SL's have been thoroughly investigated both theoretically[21–37] and experimentally.[18,38–41] For polytype SL's, however, the corresponding studies are rather scarce, although such systems provide a richer variety of possible surface configurations. Only very recently we have proposed a general formalism accounting for surface states in the electronic structure of a terminated complex-basis SL,[42] and applied it to biperiodic SL's with asymmetric-double-well and asymmetric-double-barrier bases.[42,43]

In this paper, we investigate the surface electronic structure of the so-called *step-well basis* SL, which constitutes the simplest possible polytype SL, with period consisting of three different layers. The surface-state-energy expression and the corresponding existence condition are derived for arbitrary terminating medium and the dependence of surface-state properties (i.e., its energy position and the degree of localization) on SL parameters (i.e., layer thicknesses and potential barrier heights) as well as on different surface configurations (depending on the material by which the growth sequence ends) is studied.

To the best of our knowledge, this problem has been previously addressed only by Masri and Rahmani,[44] who, however, considered just a particular GaSb/AlSb/InAs system and concentrated on possible surface states located in the main SL gap. On the contrary, we study here a general triple-constituent $Al_xGa_{1-x}As$-based SL, as this choice enables one to manipulate a wide range of potential profiles, and investigate the properties of surface states appearing within SL minigaps in the conduction-band energy range, which seems to be most important for potential device applications. Fur-

thermore, we plot the wave functions corresponding to surface states in order to investigate the associated space-charge distributions and, in particular, to show charge confinement to the SL end. In addition, the tight-binding approach used in Ref. 44 limited the layer widths considered there to a few atomic planes at most, while the effective-mass-approximation model used here applies to a complementary range of larger thicknesses of SL layers. Additionally, it enables one to obtain entirely analytical closed-form expressions on the one hand, and requires very modest computational efforts on the other.

II. MODEL

The structure under consideration is a semi-infinite step-well basis SL, described by a generalized Kronig-Penney-type model (as in the caption of Fig. 1) terminated by a potential step representing a substrate or a cladding layer. The corresponding potential profile is schematically shown in Fig. 1. The SL basis consists of three layers, labeled with A, B, and C, of thicknesses d_A, d_B, and d_C, effective-mass values m_A, m_B, and m_C, and potential barrier heights V_A, V_B, and V_C, respectively. The corresponding substrate parameters are denoted by m_S and V_S.

III. FORMALISM

Electronic structure of a terminated ternary SL is investigated using the transfer-matrix formalism within an effective-mass approximation, recently proposed to study surface effects in polytype SL's and described in detail in Ref. 42. Within this approach, explicit analytical formulas for the bulk dispersion relation as well as the energy expression and existence condition for surface states have been derived for a general complex basis and any terminating medium. However, expressions obtained for the case of an arbitrary N-layer basis appear to be rather complicated. On the contrary, applying the general formalism to a triple-constituent SL results in a significant simplification of the respective formulas, so they can be written in a quite concise manner.

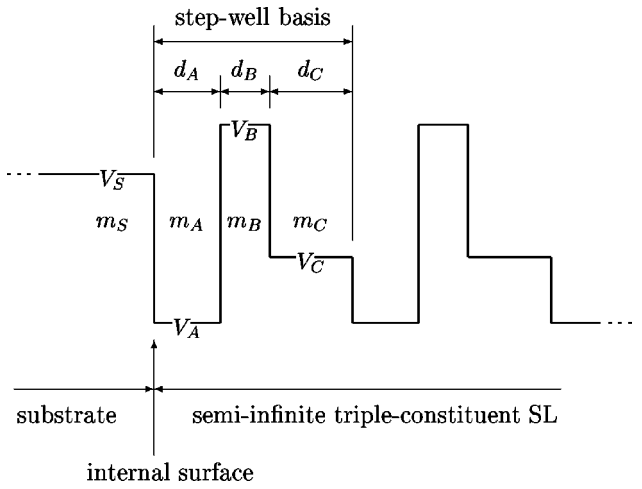

FIG. 1. Potential profile of the considered structure. Semi-infinite triple-constituent SL is described by a generalized Kronig-Penney-type model with a step-well basis, terminated by a potential step representing a substrate or a cladding layer. For notation see the text.

In particular, the bulk dispersion relation takes for a step-well basis SL a simple and closed form, namely,

$$\cos(kD)=c_Ac_Bc_C+\frac{1}{2}\left(\frac{F_A}{F_B}+\frac{F_B}{F_A}\right)s_As_Bc_C+\frac{1}{2}\left(\frac{F_A}{F_C}+\frac{F_C}{F_A}\right)s_Ac_Bs_C+\frac{1}{2}\left(\frac{F_B}{F_C}+\frac{F_C}{F_B}\right)c_As_Bs_C\equiv B_{ABC}(E). \tag{1}$$

In Eq. (1), as well as in the forthcoming expressions, $c_i=\cosh(\alpha_i d_i)$, $s_i=\sinh(\alpha_i d_i)$, and

$$F_i=\frac{\hbar^2}{2m_i}\alpha_i,$$

where

$$\alpha_i=\frac{1}{\hbar}\sqrt{2m_i(V_i-E)},\quad i=A,B,C;$$

$D=d_A+d_B+d_C$ stands for the SL period, E denotes the energy of an electron, while k is the corresponding SL Bloch wave vector.

In such a form, the bulk dispersion relation for a triple-constituent SL has already been reported (cf., e.g., Refs. 13 and 15). In particular, the miniband edges can be determined with the help of Eq. (1) by equating $B_{ABC}(E)$ to ± 1. This enables one to find the associated energy minigaps, within which discrete energy levels of surface-localized states may appear in a terminated SL.

Electronic band structure of a ternary SL can also be related to the band structures of hypothetic binary SL's built of three-layer-basis constituents. In other words, it is possible to express $B_{ABC}(E)$ [cf. Eq. (1)] in terms of $B_{AB}(E)$, $B_{AC}(E)$, and $B_{BC}(E)$, where

$$B_{AB}(E)=c_Ac_B+\frac{1}{2}\left(\frac{F_A}{F_B}+\frac{F_B}{F_A}\right)s_As_B \tag{2}$$

is the right-hand side of the bulk dispersion relation corresponding to a virtual binary SL with a basis composed of layer A and layer B (cf., e.g., Refs. 13 and 15); $B_{AC}(E)$ and $B_{BC}(E)$ are defined analogously. The respective expression reads

$$\cos(kD)=c_CB_{AB}(E)+c_BB_{AC}(E)+c_AB_{BC}(E)-2c_Ac_Bc_C. \tag{3}$$

As is apparent from Eqs. (1) and (3), the bulk dispersion relation for a step-well basis SL is invariant under any permutation of SL layers. In principle, two possible ternary SL's can be built of the same constituents, namely, the $\ldots ABCABC \ldots$ and $\ldots ACBACB \ldots$ systems.[45] But the latter sequence is the former spelled backwards—they are, therefore, indistinguishable in an *infinite* recurrence, which leads to identical electronic band structures. If a semi-infinite SL is formed, however, the two available configurations are no longer equivalent. Moreover, one can distinguish then between terminating the growth sequence at different SL constituents. Therefore, both the sequence of layers in the bulk and the type of the outermost layer have to be specified for surface electronic structure calculations of a semi-infinite ternary SL. Each of the different possible configurations may exhibit specific features—this, of course, depends also on the choice of material with which the SL makes contact.

Discrete energy levels of surface states are found within SL minigaps with the help of a general expression derived in Ref. 42 for an arbitrary terminated polytype SL. Applying it to a step-well basis yields[46]

$$\left(\frac{F_S F_B}{F_A F_C}-\frac{F_A F_C}{F_S F_B}\right)s_A s_B s_C+\left(\frac{F_S}{F_A}-\frac{F_A}{F_S}\right)s_A c_B c_C+\left(\frac{F_S}{F_B}-\frac{F_B}{F_S}\right)c_A s_B c_C+\left(\frac{F_S}{F_C}-\frac{F_C}{F_S}\right)c_A c_B s_C+\left(\frac{F_A}{F_B}-\frac{F_B}{F_A}\right)s_A s_B c_C$$
$$+\left(\frac{F_A}{F_C}-\frac{F_C}{F_A}\right)s_A c_B s_C+\left(\frac{F_B}{F_C}-\frac{F_C}{F_B}\right)c_A s_B s_C=0, \tag{4}$$

where

$$F_S=\frac{\hbar^2}{2m_S}\alpha_S,$$

while

$$\alpha_S=\frac{1}{\hbar}\sqrt{2m_S(V_S-E)}.$$

However, as pointed out in Ref. 42, the energy solution to Eq. (4)—in order to correspond to a true surface state—must additionally fulfill the following inequality

$$\left|F_S\left(\frac{s_A}{F_A}c_B c_C+\frac{s_B}{F_B}c_A c_C+\frac{s_C}{F_C}c_A c_B+\frac{F_B}{F_A F_C}s_A s_B s_C\right)\right.$$
$$\left.-\frac{F_B}{F_A}s_A s_B c_C-\frac{F_C}{F_A}s_A c_B s_C-\frac{F_C}{F_B}c_A s_B s_C-c_A c_B c_C\right|>1. \tag{5}$$

Physical meaning of this so-called existence condition is to assure a vanishing character of the surface-state wave function towards the SL bulk.

As one can see, formulas obtained for an arbitrary terminating medium are rather complicated. There are, however, particular cases, corresponding to a substrate made of the same material as one of SL constituents, for which the respective expressions can be further simplified. Such terminating conditions seem also preferred from the grower's point of view, as then the whole structure can be grown with a reduced number of different materials.

It is worth noticing that in a binary SL terminated by a step potential identical to the SL barriers (the so-called *symmetric termination* of the SL potential) surface states cannot appear as long as the outermost SL period is not distorted in any other way (cf., e.g., Ref. 38), since the corresponding existence condition is never satisfied. This restriction, however, does not hold for a semi-infinite SL with $N>2$ layers per period.[42,43] Consequently, surface states may occur in a ternary SL terminated by a substrate identical to layer-B or layer-C constituent of the step-well basis (cf. Fig. 1).

For the substrate made of the same material as layer B, $m_S=m_B$ and $V_S=V_B$ (cf. Fig. 1), and, consequently, $\alpha_S=\alpha_B$ and $F_S=F_B$. In such a case, the surface-state-energy expression [cf. Eq. (4)] reads

$$\left(\frac{F_A}{F_B}-\frac{F_B}{F_A}\right)s_A[c_C-2B_{BC}(E)e^{-\alpha_B d_B}]+\left(\frac{F_A}{F_C}-\frac{F_C}{F_A}\right)s_A s_C$$
$$+\left(\frac{F_B}{F_C}-\frac{F_C}{F_B}\right)c_A s_C=0 \tag{6a}$$

or, equivalently,

$$\left(\frac{F_B}{F_C}-\frac{F_C}{F_B}\right)s_C[c_A-2B_{AB}(E)e^{-\alpha_B d_B}]+\left(\frac{F_A}{F_B}-\frac{F_B}{F_A}\right)s_A c_C$$
$$-\left(\frac{F_A}{F_C}-\frac{F_C}{F_A}\right)s_A s_C=0, \tag{6b}$$

while the corresponding existence condition [cf. Eq. (5)] becomes

$$\left|\left(c_A c_B+\frac{F_B}{F_A}s_A s_B\right)\left(c_C-\frac{F_B}{F_C}s_C\right)\right.$$
$$\left.-\left(c_A s_B+\frac{F_B}{F_A}s_A c_B\right)\left(c_C-\frac{F_C}{F_B}s_C\right)\right|>1. \tag{7}$$

Furthermore, since Eq. (7) is to be satisfied just for the solutions of Eq. (6a) or (6b), we make use of Eqs. (6) and arrive at

$$|2[B_{AB}(E)-c_Ac_B][B_{BC}(E)-c_Bc_C]+B_{AC}(E) - B_{ABC}(E)e^{-\alpha_B d_B}|>|s_B| \quad (8)$$

as another form of the necessary condition for a surface state to appear in a ternary SL terminated by a medium identical to the central constituent layer of the SL basis.

For the substrate made of the same material as layer C, $m_S=m_C$ and $V_S=V_C$ (cf. Fig. 1), so $\alpha_S=\alpha_C$, and Eqs. (4) and (5) can be substantially simplified by putting $F_S=F_C$. Indeed, after such a substitution, the energy expression for surface states [cf. Eq. (4)] and the corresponding existence condition [cf. Eq. (5)] reduce to

$$\left(\frac{F_A}{F_C}-\frac{F_C}{F_A}\right)s_Ac_B+\left(\frac{F_B}{F_C}-\frac{F_C}{F_B}\right)c_As_B-\left(\frac{F_A}{F_B}-\frac{F_B}{F_A}\right)s_As_B=0 \quad (9)$$

and

$$\left|\frac{F_B}{F_A}s_As_B-\frac{F_C}{F_A}s_Ac_B-\frac{F_C}{F_B}c_As_B+c_Ac_B\right|>e^{\alpha_C d_C}, \quad (10)$$

respectively. By combining Eqs. (9) and (10), another simple form of the necessary condition for a surface state to occur in a ternary SL terminated by a medium identical to the last constituent layer of the SL basis immediately follows, namely,

$$|B_{AB}(E)-B_{ABC}(E)e^{-\alpha_C d_C}|>|s_C|. \quad (11)$$

A striking property of this particular termination, apparent from Eq. (9), is that the surface-state energies do not depend on the thickness d_C of layer C. Moreover, Eq. (9) is exactly the energy expression for surface states in a binary SL composed of layer A and layer B, and terminated by the substrate with $m_S=m_C$ and $V_S=V_C$. This means that solutions to the surface-state-energy expression are the same for SL's with and without the third constituent in the basis. One should have in mind, however, that solutions of Eq. (9) correspond to true surface-state energies provided the existence condition is satisfied. But Eq. (10) does not reproduce the respective condition for a binary SL with the layer-A/layer-B basis being in contact with the substrate with $m_S=m_C$ and $V_S=V_C$ [it would, if the right-hand side of Eq. (10) were equal to 1]. On the contrary, it indicates a critical dependence of the surface-state occurrence in a triple-constituent SL on the thickness of layer C. In particular, for d_C large enough Eq. (10) is not fulfilled, so surface states cannot appear.

Anyway, we can conclude that as long as the surface state exists in a ternary SL, its energy position is independent of the width of the last layer composing the SL basis, whenever this layer is identical to the substrate. This, in fact, illustrates a more general peculiarity of polytype SL's terminated by the same medium as the last complex-basis constituent, as has been thoroughly discussed in Ref. 42.

For any energy solution to Eq. (4), (6), or (9), the corresponding wave function can also be constructed, following a general prescription given in Ref. 42. Unfortunately, even for a polytype SL as simple as the triple-constituent one, no concise analytical formulas for the surface-state wave function can be reached, so it has to be entirely determined numerically.

IV. NUMERICAL RESULTS

For numerical calculations, the $Al_xGa_{1-x}As$-based system has been chosen, as it exhibits excellent growth characteristics and enables one to realize and manipulate a wide range of potential profiles. In such a structure, the potential barrier height and the effective-mass value of a given region are determined by the Al mole fraction x_i in the corresponding $Al_{x_i}Ga_{1-x_i}As$ semiconductor ($i=A$, B, and C for the SL layers and $i=S$ for the substrate) according to $V_i(x_i)=944x_i$ meV and $m_i(x_i)=(0.067+0.083x_i)m_{el}$, respectively, m_{el} being the free-electron mass (after Ref. 18).

It should be noticed that the surface electronic structure is investigated only for energies up to the substrate potential, i.e., for $E<V_S$, since above this level true bound states can no longer exist. On the other hand, this energy range is particularly interesting from the point of view of possible device applications, as it usually comprises the lowest and, eventually, the second energy miniband.

As a first step, the influence of variation of different layer thicknesses on the electronic structure of a step-well basis SL is studied. To this aim, we fix all the other structure parameters—in particular, the semiconductors composing the SL are settled by assuming $x_A=0$ (layer A made of GaAs), $x_B=1$ (layer B made of AlAs), and $x_C=0.5$ (layer C made of $Al_{0.5}Ga_{0.5}As$). This results in $m_A=0.067m_{el}$, $V_A=0$, $m_B=0.15m_{el}$, $V_B=944$ meV, $m_C=0.1085m_{el}$, and $V_C=472$ meV. Thicknesses of all the constant-width layers are equal to 20 Å. Various surface conditions are taken into account by considering two different substrates, namely, AlAs (substrate identical to layer B) and $Al_{0.5}Ga_{0.5}As$ (substrate identical to layer C). Consequently, $x_S=x_B=1$ or $x_S=x_C=0.5$, leading to $m_S=m_B=0.15m_{el}$ and $V_S=V_B=944$ meV or $m_S=m_C=0.1085m_{el}$ and $V_S=V_C=472$ meV, respectively.

Results of the surface electronic structure computations, which take into account different possible configurations of layers in the SL basis, are presented in Figs. 2 and 3 for the substrate identical to layer C and layer B, correspondingly. In each of these figures, parts (a), (b), and (c) show the effect of variable d_A, d_B, and d_C, respectively, with all the remaining thicknesses kept constant.

As can be seen in Figs. 2(a) and 3(a), increasing the thickness d_A of layer A causes a shift downwards in energy and a simultaneous narrowing of the otherwise narrow lowest miniband. This can be easily understood if one has in mind that the first miniband falls into the energy range $E<V_C$, where the electronic structure is predominantly determined by the width-sensitive eigenspectrum of a deep quantum well formed by layer A inside a bigger potential well of joint layer A and layer C (cf. Fig. 1). Figure 3(a) indicates basically the same behavior of the second miniband, which is already located entirely above V_C, resulting from a broadening of the step well as a whole.

On the contrary, varying the width d_B of layer B leaves

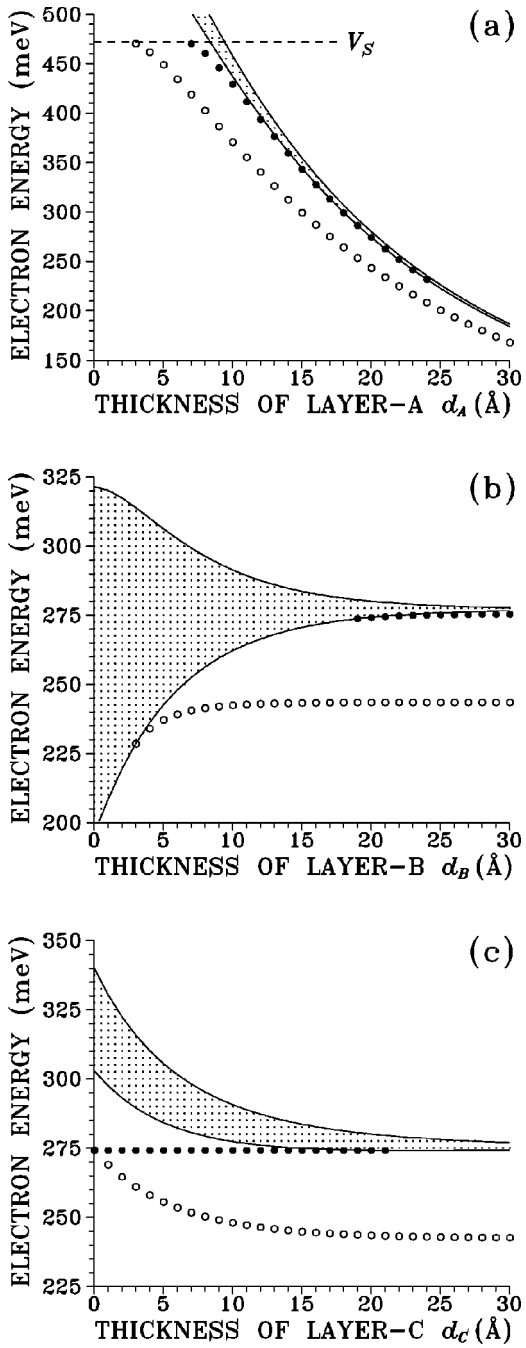

FIG. 2. Influence of different layer thickness variation on the electronic structure of a step-well basis SL with $x_A=0$, $x_B=1$, and $x_C=0.5$, terminated by a substrate identical to layer C ($x_S=0.5$): (a) d_A variable, $d_B=d_C=20$ Å; (b) d_B variable, $d_A=d_C=20$ Å; (c) d_C variable, $d_A=d_B=20$ Å. Shaded areas correspond to the minibands while full dots and open circles indicate the position of surface states for the substrate/$ABCABC\ldots$ and substrate/$ACBACB\ldots$ configuration, respectively (no surface states appear for the substrate/$BACBAC\ldots$ and substrate/$BCABCA\ldots$ sequences). Dashed line in part (a) denotes the surface potential level V_S.

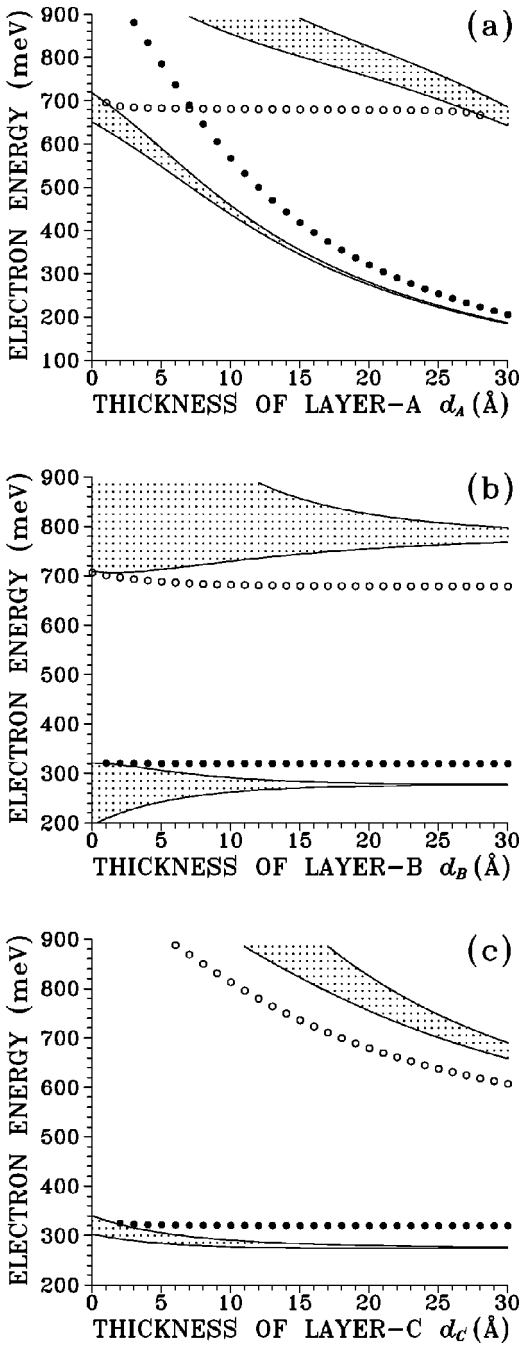

FIG. 3. The same as in Fig. 2, but for a substrate identical to layer B ($x_S=1$). Full dots and open circles indicate the position of surface states for the substrate/$ABCABC\ldots$ and substrate/$CBACBA\ldots$ configuration, respectively, while no surface states appear for the substrate/$ACBACB\ldots$ and substrate/$CABCAB\ldots$ sequences.

the first-miniband-center position virtually unchanged, but dramatically influences its bandwidth [cf. Figs. 2(b) and 3(b)]. Such a significant miniband narrowing is, in fact, expected for increasing the thickness, i.e., decreasing the transparency, of the SL barriers (please keep in mind that both layer B and layer C act as a potential barrier for $E<V_C$). For the upper miniband a similar, but less pronounced, effect is observed [cf. Fig. 3(b)], since for $E>V_C$ layer B alone stands for the SL barrier.

Finally, changing the thickness d_C of layer C again causes a movement of the first miniband towards lower energies [cf. Figs. 2(c) and 3(c)], which can be explained in terms of a simple potential-profile-picture argument. Introducing layer C into the SL basis creates a medium-height potential stair at one of the steep walls formed at the interfaces between layer

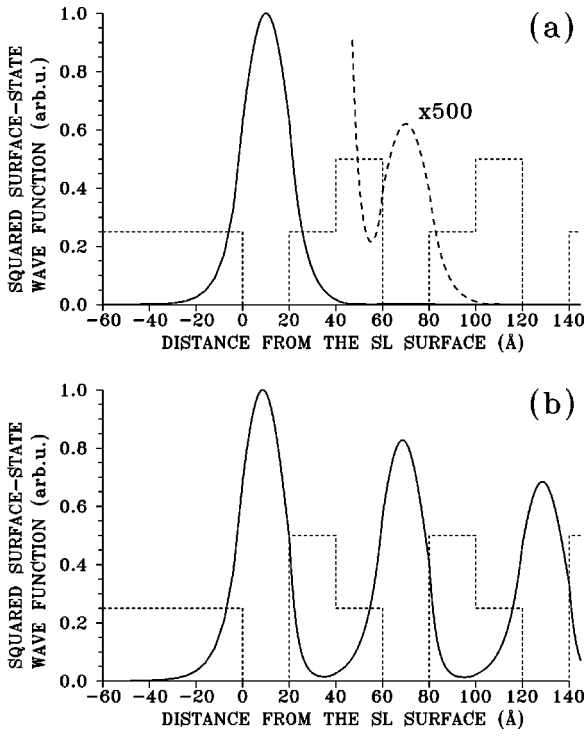

FIG. 4. Squared wave functions (normalized to reach a maximum value of 1) of surface states corresponding to (a) substrate/$ACBACB\ldots$ and (b) substrate/$ABCABC\ldots$ configuration of layers of a step-well basis SL with $x_A=0$, $x_B=1$, $x_C=0.5$, and $d_A=d_B=d_C=20$ Å, terminated by a substrate with $x_S=0.5$, i.e., identical to layer C (solid lines). Short-dashed lines depict schematically the respective potential profiles, while the long-dashed curve in part (a) represents the wave function enlarged within the second SL period.

A and layer B (cf. Fig. 1). As a result, the eigenstates of a quantum well of layer A are slightly shifted downwards in energy. This effect reaches a kind of saturation for greater potential-step widths—therefore, for large enough d_C ($d_C \gtrsim 20$ Å) the lowest miniband position remains essentially unchanged [cf. Figs. 2(c) and 3(c)]. The respective bandwidth reduction again is a straightforward consequence of enlarging the quantum potential barrier of joint layer B and layer C. Dependence of the second miniband on d_C [cf. Fig. 3(c)] resembles—to a large extent—the effect of variable d_A [cf. Fig. 3(a)], as the band structure in the energy range $E > V_C$ originates from intermixed eigenstates of layer A and layer C.

As expected, terminating the SL potential introduces additional energy levels inside energy minigaps, corresponding to the states localized at the SL end. However, not all available configurations of SL layers provide surface states. To be more specific, for the substrate identical to layer C they only occur if layer A stands for the outermost SL layer, while no surface-related features are present in the spectrum for the substrate/$BCABCA\ldots$ and substrate/$BACBAC\ldots$ sequences (cf. Fig. 2). On the contrary, for the substrate identical to layer B surface states appear for either layer A or layer C being in contact with substrate (cf. Fig. 3).

For the $Al_{0.5}Ga_{0.5}As$ substrate, since $V_S=V_C$, surface-localized levels only exist in the energy range $E<V_C$, i.e., within a quantum well corresponding to layer A, while joint layer B and layer C act as a steplike potential barrier (cf. Fig. 1). This geometry influences most features of the surface states and, in particular, determines their space-charge distributions. As can be seen in Fig. 2, for the substrate identical to layer C all the surface-state-energy curves appear *below* the first miniband, since the terminating potential step is *lower* than an average potential barrier inside the SL, in accordance with earlier findings for semi-infinite binary SL's (cf., e.g., Refs. 27 and 29). Moreover, surface states corresponding to the substrate/$ACBACB\ldots$ sequence have always smaller energies than those of the substrate/$ABCABC\ldots$ configuration—this is because the outermost layer A, if treated as an isolated quantum well, has its ground eigenstate at a lower energy when cladded on both sides by potential barriers of a smaller height V_C.

When the width d_A of layer A is increased, both surface-state-energy curves fall down in energy following the miniband variation [cf. Fig. 2(a)]. One of the surface states, corresponding to the substrate/$ACBACB\ldots$ sequence, remains clearly separated from the miniband edge for the whole range of considered layer-A thicknesses. Analysis of its wave function, plotted in Fig. 4(a) for $d_A=20$ Å, indicates a strong confinement to the outermost SL layer with the squared-wave-function amplitude decaying by a factor as large as 800 in each subsequent SL period as one moves off the SL surface. Consequently, any electron in such a state would be, in fact, captured in a *single* subsurface potential well. The other surface state, corresponding to the substrate/$ABCABC\ldots$ configuration, lies much closer to the miniband edge and approaches it with increasing d_A—therefore, its localization at the SL surface is getting poorer and poorer.[47] In particular, for $d_A=20$ Å this surface state exhibits already a Bloch-like character with almost no damping towards the SL bulk, as is apparent from the shape of its wave function shown in Fig. 4(b). Eventually, for $d_A \approx 25$ Å it merges into the miniband and ceases to exist.

A similar surface state approaching the lowest energetic miniband has been reported in Ref. 44 for a semi-infinite GaSb/AlSb/InAs SL terminated at the In-cation plane. As has been noticed, transfer of electrons to such a surface-localized level—though it can hardly be separated from the miniband-associated bulk transitions—results in a charge confinement to the SL end and, therefore, might have important consequences for specific electronic characteristics.

The effect of varying the thickness d_B of layer B is presented in Fig. 2(b). As expected, no surface states exist for $d_B=0$, since then our structure becomes a binary layer-A/layer-C SL terminated in a symmetric way. However, a surface state appears for layer B as thin as a few angströms for the substrate/$ACBACB\ldots$ configuration. On the other hand, that corresponding to the substrate/$ABCABC\ldots$ sequence detaches from the miniband only at $d_B \approx 20$ Å. Energies of both of them are almost insensitive to the variation of d_B, but increasing the SL barrier thickness enhances their confinement to the SL end. Of course, each of the surface states exhibits a different degree of localization (cf. Fig. 4 for the corresponding wave functions plotted for $d_B=20$ Å) due to a distinct energy separation from the miniband edge.[47]

Figure 2(c) shows a dependence of surface-state-energy curves on the width d_C of layer C. As can be seen, in the limit of $d_C=0$ both of them reach the same energy level,

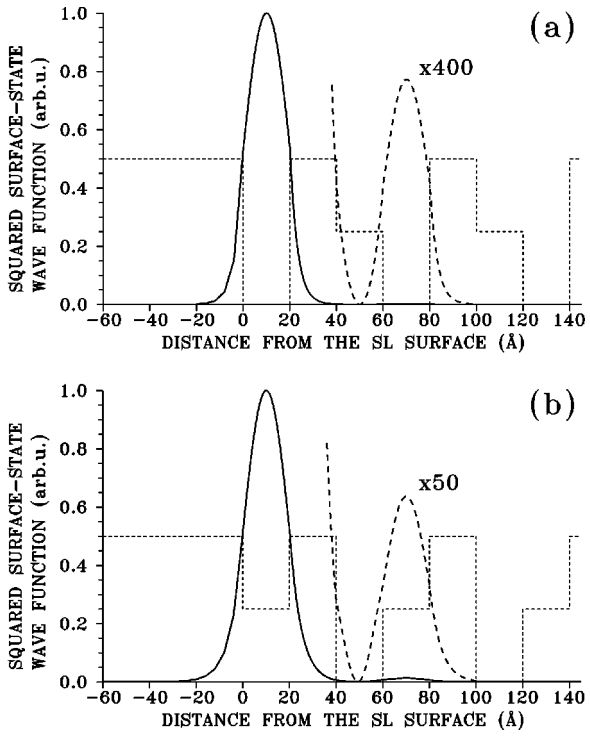

FIG. 5. The same as in Fig. 4, but for a substrate identical to layer B ($x_S=1$) and for (a) substrate/$ABCABC\ldots$ and (b) substrate/$CBACBA\ldots$ sequence of SL layers.

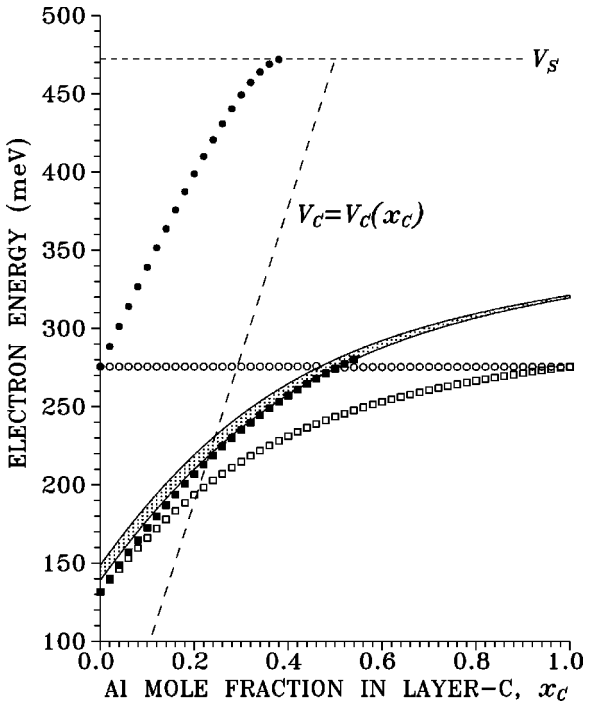

FIG. 6. Influence of variation of the Al mole fraction in layer C, x_C, on the electronic structure of a step-well basis SL with $x_A=0$, $x_B=1$, and $d_A=d_B=d_C=20$ Å, terminated by a substrate with $x_S=0.5$. The shaded area corresponds to the lowest miniband. Full dots and squares indicate the position of surface states for the substrate/$CBACBA\ldots$ and substrate/$CABCAB\ldots$ configuration, while open circles and squares—for the substrate/$ABCABC\ldots$ and substrate/$ACBACB\ldots$ sequence, correspondingly (no surface states appear for the substrate/$BACBAC\ldots$ and substrate/$BCABCA\ldots$ configurations). Short- and long-dashed lines denote the surface potential level V_S and the potential stair height V_C, respectively.

corresponding to the surface state of a binary layer-A/layer-B terminated by a potential step V_C. With increasing d_C, the substrate/$ACBACB\ldots$ configuration-derived surface state falls down in energy in the same way (and for the same reason) as the lowest miniband does, which results in a basically constant energy separation from the miniband edge. On the contrary, the energy position of a surface state corresponding to the substrate/$ABCABC\ldots$ is completely independent of the layer-C thickness, so it relatively approaches the falling miniband. This agrees with Eq. (9) and clearly illustrates the already discussed (cf. Sec. III) peculiar behavior of surface states of a ternary SL terminated by the same medium as the last constituent of the SL basis. For d_C large enough ($d_C\approx 20$ Å) this surface state merges into the miniband and—in accordance with Eq. (10)—ceases to exist.

As can be seen in Fig. 3, altering the terminating conditions by taking the AlAs substrate (identical to layer B) instead of the $Al_{0.5}Ga_{0.5}As$ one (identical to layer C), influences quite noticeably the surface electronic structure of the considered triple-constituent SL. In particular, configurations of layers of the step-well basis, for which surface-localized levels occur, change. To be more specific, the substrate/$ACBACB\ldots$ geometry no longer exhibits any surface-related features in the spectrum, and neither does the substrate/$CABCAB\ldots$ one. The substrate/$ABCABC\ldots$ sequence, however, again provides a surface state. Moreover, its dependence on the width of particular SL layers is similar to that observed for the $Al_{0.5}Ga_{0.5}As$ substrate: it falls down in energy with increasing d_A, while varying d_B and d_C has a negligible effect on its energy position [cf. Figs. 3(a), 3(b), and 3(c) versus Figs. 2(a), 2(b), and 2(c), respectively]. But this time it exists, in fact, for the whole range of considered layer thicknesses. In addition, the respective surface-state-energy curves appear now *above* the lowest miniband, since the terminating potential step for the AlAs substrate is *higher* than an average potential barrier inside the SL (cf., e.g., Refs. 27 and 29). The corresponding surface-state wave function, plotted in Fig. 5(a) for $d_A=d_B=d_C=20$ Å, resembles that of Fig. 4(b)—the only changes concern, in fact, a different degree of localization. Here, we again deal with a state almost *completely* confined to the single outermost SL layer.

Another surface state, absent in Fig. 2, occurs at higher energies for the substrate/$CBACBA\ldots$ configuration (note that the energy range $V_C<E<V_B$ becomes now available for surface-localized levels, since $V_S=V_B$ for the AlAs substrate). Its energy position is almost insensitive to the variation of d_A and d_B, as is apparent from Figs. 3(a) and 3(b), respectively. Changing the width d_C of layer C, however, causes the corresponding surface-state-energy curve to fall down in energy, in accordance with the second miniband variation [cf. Fig. 3(c)]. Additionally, since for the substrate/$CBACBA\ldots$ geometry the outermost layer C is cladded on both sides by layer-B material, hence creating a potential well of depth (V_B-V_C) and width d_C in the subsurface SL region, a surface state corresponding to such terminating conditions is assumed to originate from a layer-C-associated eigenstate. To confirm such character of this surface state, its wave function has been plotted in Fig. 5(b)

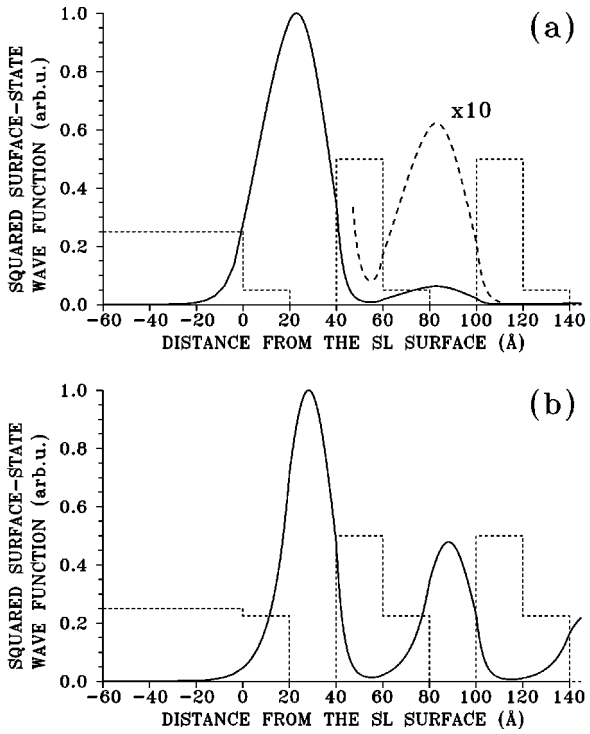

FIG. 7. Squared wave functions (normalized to reach a maximum value of 1) of a surface state corresponding to the substrate/$CABCAB\ldots$ configuration of layers of a step-well basis SL with $d_A=d_B=d_C=20$ Å, $x_A=0$, $x_B=1$, and (a) $x_C=0.1$ and (b) $x_C=0.45$, terminated by a substrate with $x_S=0.5$ (solid lines). Short-dashed lines depict schematically the respective potential profiles, while the long-dashed curve in part (a) represents the wave function enlarged within the second SL period.

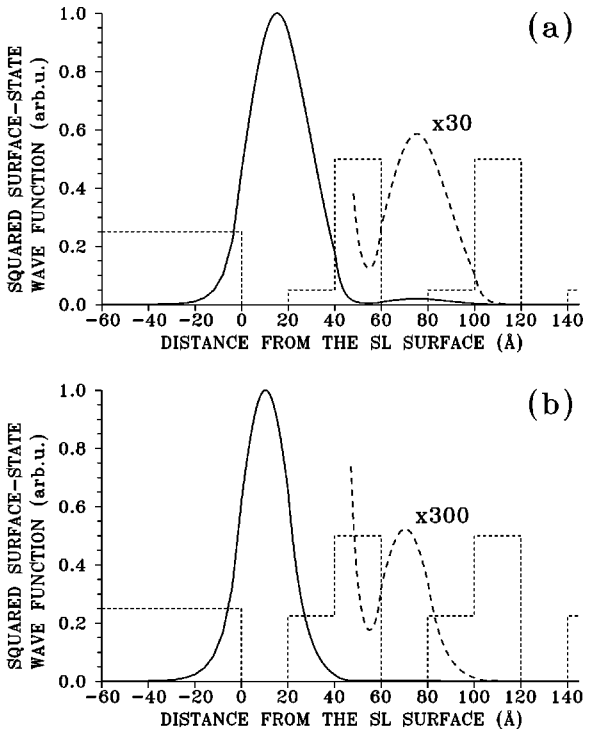

FIG. 8. The same as in Fig. 7, but for a surface state corresponding to the substrate/$ACBACB\ldots$ sequence of SL layers.

for $d_A=d_B=d_C=20$ Å. As can be clearly seen, it is indeed predominantly localized in the outermost quantum well; moreover, within each step-well SL period it exhibits a maximum in layer C rather than in layer A, in contrast to a surface state corresponding to the substrate/$ABCABC\ldots$ configuration [cf. Fig. 5(b) versus Fig. 5(a)].

It should be pointed out that if a SL consists of a *finite* number of periods, two surfaces are created, so two surface states, confined to distinct SL ends, can appear in the electronic structure (cf., e.g., Ref. 37). In a polytype SL, both surfaces might differ not only by substrate parameters, but also by a sequence of layers approaching the surface. For instance, when the substrate/$ABCABC\ldots$ configuration is formed at one end of a triple-constituent SL, the substrate/$CBACBA\ldots$ geometry corresponds to the other end. However, as follows from Fig. 3(a), for appropriately chosen SL and substrate parameters, the surface-state-energy curves corresponding to these sequences may cross each other [cf. Fig. 3(a) for $d_A\approx 7$ Å]. Since both surface states would interact with one another, exhibiting a mixed character with nonzero amplitudes at either of the SL ends, an interesting anticrossing behavior should be observed for selected layer thicknesses. This effect, of course, depends on an overlap of their wave functions, and thus—in principle—can be tuned by varying the degree of localization of individual surface states.

Another way of modifying the geometry of the SL step-well basis is to change the potential stair height while keeping all the layer thicknesses constant. This can be done, e.g., by varying the Al mole fraction x_C in layer C within the limits set by fixed x_A and x_B. The resulting effect on the surface electronic structure is illustrated in Fig. 6 for a SL with $d_A=d_B=d_C=20$ Å, $x_A=0$, $x_B=1$, and substrate parameters corresponding to $x_S=0.5$.

For such a system, only the lowest miniband falls into the investigated energy range $E<V_S$. Increasing x_C (i.e., increasing V_C) causes its shift upwards in energy, in accordance with a similar behavior of the ground eigenstate of a corresponding isolated step quantum well. Additionally, a miniband narrowing is observed due to a decreasing transparency of the SL barriers.

As can be seen in Fig. 6, only four SL layer configurations (out of six possible) provide surface states. In particular, no surface-related features occur in the spectrum if the SL is terminated at layer B. Moreover, those corresponding to the SL termination at layer C appear only for $V_C \lesssim V_S$. This indicates that—in order to obtain a surface state—the potential of the outermost SL layer *must not* be significantly higher than the substrate potential. In other words, the existence of a well-defined surface state depends on the formation of a potential well in the subsurface SL region. In support of this, both the substrate/$ABCABC\ldots$ and substrate/$ACBACB\ldots$ sequences provide surface states for the whole range of considered parameters.

Each of the surface-state-energy curves plotted in Fig. 6 exhibits a different behavior. Those corresponding to the substrate/$ACBACB\ldots$ and substrate/$CABCAB\ldots$ configurations are located entirely beneath the first miniband. In the limit of $x_C=0$, they converge to the position of a surface state of the substrate/$AABAAB\ldots$ system (cf. Fig. 1), i.e., the binary (40 Å)–GaAs/(20 Å)–AlAs SL terminated by the $Al_{0.5}Ga_{0.5}As$ substrate. With increasing x_C, the

substrate/$CABCAB\ldots$ configuration-derived surface state follows the miniband variation, gradually approaching the miniband edge. This causes its wave function [shown in Figs. 7(a) and 7(b) for $x_C=0.1$ and $x_C=0.45$, respectively] to delocalize. Finally, for $x_C\approx 0.55$ it merges into the miniband and ceases to exist.

On the contrary, a surface state corresponding to the substrate/$ACBACB\ldots$ sequence occurs for all values of x_C. Considerable energy separation from the miniband bottom results in a strong localization of its wave function at the SL end, as illustrated in Fig. 8. In each of Figs. 7 and 8, changes of the respective surface-state-associated charge distribution over the SL period can additionally be seen: a broad wave-function maximum extending over layer *A and* layer *C* for $x_C \lesssim 0.2$ [cf. Figs. 7(a) and 8(a)] gets confined *solely* to layer *A* for larger values of x_C [cf. Figs. 7(b) and 8(b)]. For $x_C=1$, when the substrate/$ACBACB\ldots$ sequence becomes the substrate/$ABBABB\ldots$ one (cf. Fig. 1), the corresponding surface state reproduces that of the binary (20 Å)–GaAs/(40 Å)–AlAs SL terminated by the $Al_{0.5}Ga_{0.5}As$ substrate.

The same holds, in this limit, for a surface state of the substrate/$ABCABC\ldots$ configuration. As can be seen in Fig. 6, its energy position is, in practice, insensitive to the Al mole fraction variation in layer *C*. Around $x_C=0.5$, this surface state crosses the bulk miniband.[48] As a consequence, it ceases to exist for a small range of x_C values and reappears above the miniband for $x_C \lesssim 0.47$. Eventually, for $x_C=0$, the surface state of the substrate/$ABCABC\ldots$ configuration coincides with that of the substrate/$CBACBA\ldots$ sequence, as then each of them corresponds to the substrate/$ABAABAA\ldots$ system (cf. Fig. 1), i.e., the semi-infinite binary (40 Å)–GaAs/(20 Å)–AlAs SL with the outermost GaAs quantum well two times narrower than the interior ones (the so-called *embedded quantum well*[38]).

Finally, the surface-localized level provided by the substrate/$CBACBA\ldots$ configuration appears in the higher-energy region only for $x_C \lesssim 0.4$ and is roughly pinned to the potential step height V_C. As already discussed, its wave function is predominantly confined to the outermost layer *C* and, within each step-well SL period, exhibits a maximum in layer *C* rather than in layer *A*, in contrast with all the remaining surface states.

V. SUMMARY

In this work, using a transfer-matrix method within an envelope-function approximation (cf. Ref. 42), the electronic structure of a semi-infinite step-well basis SL has been investigated, with emphasis placed on the effect of the SL surface (i.e., the SL/substrate interface). Explicit analytical formulas for the bulk dispersion relation as well as the energy expression and existence condition for surface-localized states have been derived for arbitrary terminating medium. Special attention has been paid to particular SL terminations by a substrate identical to one of the SL constituents—in such cases, the respective expressions have been substantially simplified.

Dependence of the surface electronic structure on SL parameters (i.e., layer thicknesses and potential barrier heights) as well as on different surface configurations (depending on the choice of substrate and the sequence of SL layers approaching the surface) has been discussed in detail based on results of numerical computations performed for $Al_xGa_{1-x}As$-based ternary SL's. A different behavior of surface-localized states with respect to bulk states has been noticed along with a significant sensitivity of their properties to the changes in the step-well geometry. Some general conclusions concerning the occurrence of particular surface states as well as some ideas about their origin have been presented. It has been shown that a surface state with a desired energy position within the minigap and a required extension into the SL can be achieved by an appropriate choice of bulk and surface SL parameters. Selected surface-state wave functions have also been plotted in order to investigate the space-charge distributions associated with particular surface states and to indicate the degree of their localization at the SL end.

As expected, different possible terminating configurations of the SL layers (in general, six of them are available for a triple-constituent SL, with two sequences associated with each outermost layer) have been found to exhibit specific surface-related features, depending additionally on the choice of material with which the SL makes contact. It should be noticed, however, that introduction of the third layer into the SL basis and its position in a sequence of SL layers is not just a supplementary factor influencing the energies and localization properties of surface states, as compared to typical binary SL's. Indeed, in contrast to the latter, the triple-constituent SL offers a possibility of surface-state existence also for the substrate identical to the SL barriers.

Finally, it should be pointed out that—since the step-well geometry is gradually becoming a prefered design for specific opto-electronic devices exhibiting superior performance—the appearance of allowed energy levels in the otherwise forbidden energy regions of minigaps and the consequent possible electronic transitions to surface-localized states are in itself of particular interest and merit experimental investigation. Moreover, owing to optical peculiarities of SL surface states (e.g., large Stark shifts and enhanced absorption[26]) as well as a considerable tunability of their unusual properties, such levels may find useful applications.

ACKNOWLEDGMENTS

Two of us (R. K. and M. S.) would like to acknowledge support by the University of Wrocław under Grant No. 2016/W/IFD/97.

*Author to whom correspondence should be addressed. Electronic address: rku@ifd.uni.wroc.pl

[1] L. Esaki, L. L. Chang, and E. E. Mendez, Jpn. J. Appl. Phys. **20**, L529 (1981).

[2] K. K. Choi, B. F. Levine, C. G. Bethea, J. Walker, and R. J. Malik, Phys. Rev. Lett. **59**, 2459 (1987).

[3] P.-F. Yuh and K. L. Wang, Appl. Phys. Lett. **51**, 1404 (1987).

[4] P.-F. Yuh and K. L. Wang, J. Appl. Phys. **65**, 4377 (1989).

[5] A. Tomita, J. Appl. Phys. **77**, 2029 (1995).

[6] T. K. Woodward, J. E. Cunningham, and W. Y. Jan, J. Appl. Phys. **78**, 1411 (1995).

[7] K. Fujiwara, S. Hinooda, and K. Kawashima, Appl. Phys. Lett. **71**, 113 (1997).
[8] T. Mei, G. Karunasiri, and S. J. Chua, Appl. Phys. Lett. **71**, 2017 (1997).
[9] P.-F. Yuh and K. L. Wang, Phys. Rev. B **38**, 13 307 (1988).
[10] K. L. Wang and P.-F. Yuh, IEEE J. Quantum Electron. **QE-25**, 12 (1989).
[11] F. M. Peeters and P. Vasilopoulos, Appl. Phys. Lett. **55**, 1106 (1989).
[12] P. Vasilopoulos, F. M. Peeters, and D. Aitelhabti, Phys. Rev. B **41**, 10 021 (1990).
[13] G. Bastard, Phys. Rev. B **25**, 7584 (1982).
[14] H. X. Jiang and J. Y. Lin, Phys. Rev. B **33**, 5851 (1986).
[15] B. Djafari-Rouhani and L. Dobrzynski, Solid State Commun. **62**, 609 (1987).
[16] J.-J. Shi and S.-H. Pan, Phys. Rev. B **48**, 8136 (1993).
[17] L. Fernández-Alvarez, G. Monsivais, and V. R. Velasco, J. Phys.: Condens. Matter **8**, 8859 (1996).
[18] H. Ohno, E. E. Mendez, J. A. Brum, J. M. Hong, F. Agulló-Rueda, L. L. Chang, and L. Esaki, Phys. Rev. Lett. **64**, 2555 (1990).
[19] I. E. Tamm, Phys. Z. Sowjetunion **1**, 733 (1932).
[20] S. G. Davison and M. Stęślicka, *Basic Theory of Surface States* (Clarendon Press, Oxford, 1992).
[21] R. Kucharczyk and M. Stęślicka, Solid State Commun. **84**, 727 (1992).
[22] M. Stęślicka and R. Kucharczyk, Vacuum **45**, 211 (1994).
[23] V. Milanović, Physica B **121**, 181 (1983).
[24] P. Masri, L. Dobrzynski, B. Djafari-Rouhani, and J. O. A. Idiodi, Surf. Sci. **166**, 301 (1986).
[25] M. Stęślicka, R. Kucharczyk, and M. L. Glasser, Phys. Rev. B **42**, 1458 (1990).
[26] J. Zhang, S. E. Ulloa, and W. L. Schaich, Phys. Rev. B **43**, 9865 (1991).
[27] W. L. Bloss, Phys. Rev. B **44**, 8035 (1991).
[28] P. Masri, Surf. Sci. Rep. **19**, 1 (1993).
[29] E.-H. El Boudouti, R. Kucharczyk, and M. Stęślicka, Czech. J. Phys. **43**, 899 (1993).
[30] R. H. Yu, Phys. Rev. B **47**, 1379 (1993).
[31] H. K. Sy and T. C. Chua, Phys. Rev. B **48**, 7930 (1993).
[32] J. Arriaga, F. García-Moliner, and V. R. Velasco, Prog. Surf. Sci. **42**, 271 (1993).
[33] R. Kucharczyk and M. Stęślicka, Prog. Surf. Sci. **46**, 225 (1994).
[34] S. Fafard, Phys. Rev. B **50**, 1961 (1994).
[35] M. Stęślicka, R. Kucharczyk, E.-H. El Boudouti, B. Djafari-Rouhani, M. L. Bah, A. Akjouj, and L. Dobrzynski, Vacuum **46**, 459 (1995).
[36] M. Stęślicka, Prog. Surf. Sci. **50**, 65 (1995).
[37] S.-D. Chen, C. Narayan, and A. S. Karakashian, Physica B **228**, 239 (1996).
[38] F. Agulló-Rueda, E. E. Mendez, H. Ohno, and J. M. Hong, Phys. Rev. B **42**, 1470 (1990).
[39] H. Ohno, E. E. Mendez, A. Alexandrou, and J. M. Hong, Surf. Sci. **267**, 161 (1992).
[40] T. Miller and T.-C. Chiang, Phys. Rev. Lett. **68**, 3339 (1992).
[41] G. N. Henderson, L. C. West, T. K. Gaylord, C. W. Roberts, E. N. Glytsis, and M. T. Asom, Appl. Phys. Lett. **62**, 1432 (1993).
[42] E.-H. El Boudouti, B. Djafari-Rouhani, A. Akjouj, L. Dobrzynski, R. Kucharczyk, and M. Stęślicka, Phys. Rev. B **56**, 9603 (1997).
[43] R. Kucharczyk, M. Stęślicka, E.-H. El Boudouti, A. Akjouj, L. Dobrzynski, and B. Djafari-Rouhani, Czech. J. Phys. **47**, 421 (1997).
[44] P. Masri and M. D. Rahmani, Phys. Rev. B **40**, 1175 (1989). The same results have also been reviewed by P. Masri in Ref. 28.
[45] In practice, growing of $Al_xGa_{1-x}As$ layer after GaAs layer, and followed by AlAs layer is a preferred sequence for AlGaAs-based ternary SL's, as $Al_xGa_{1-x}As$ tends to form relatively rough surfaces, while AlAs has a smoothing effect on the surface before GaAs is grown again [after D. J. Lockwood, R. L. S. Devine, A. Rodriguez, J. Mendialdua, B. Djafari-Rouhani, and L. Dobrzynski, Phys. Rev. B **47**, 13 553 (1993)].
[46] Please note that Eq. (4) as well as all the subsequent expressions correspond to the substrate/$ABCABC\ldots$ configuration of a terminated ternary SL (cf. Fig. 1).
[47] A similar critical dependence of the surface-state localization properties on its energy separation from the miniband edge as well as on the minigap-to-miniband width ratio has been observed in binary SL's (cf., e.g., Refs. 27 and 29).
[48] For a detailed discussion of the effect of a miniband crossing by a surface state (in binary SL's) see, e.g., Refs. 29 and 33.